Research Article

Received: 9 October 2018 Revised: 3 January 2019 Accepted article published: 31 January 2019 Published online in Wiley Online Library: 15 March 2019

(wileyonlinelibrary.com) DOI 10.1002/pi.5787

A biopolymer-based 3D printable hydrogel for toxic metal adsorption from water

Gayan A Appuhamillage, Danielle R Berry, Candace E Benjamin, Michael A Luzuriaga, John C Reagan, Jeremiah J Gassensmith* and Ronald A Smaldone*

Abstract

Herein, we describe a 3D printable hydrogel that is capable of removing toxic metal pollutants from aqueous solution. To achieve this, shear-thinning hydrogels were prepared by blending chitosan with diacrylated Pluronic F-127 which allows for UV curing after printing. Several hydrogel compositions were tested for their ability to absorb common metal pollutants such as lead, copper, cadmium and mercury, as well as for their printability. These hydrogels displayed excellent metal adsorption with some examples capable of up to 95% metal removal within 30 min. We show that 3D printed hydrogel structures that would be difficult to fabricate by conventional manufacturing methods can adsorb metal ions significantly faster than solid objects, owing to their higher accessible surface areas.

Supporting information may be found in the online version of this article.

Keywords: 3D printing; chitosan; biopolymer; hydrogels; water purification

INTRODUCTION

Fresh water is a basic human need, as well as a critical component for agricultural and commercial industries. However, population growth places strain on local sources of fresh water through increased usage and pollution originating from industrial waste and decaying urban infrastructure. The cost for cleanup can be prohibitively high or politically difficult, leaving few viable options for those in poor or remote locations. Water contaminants, often associated with industrial pollution, include toxic heavy metal ions such as lead, mercury, cadmium and copper. These metals can have severe and persistent effects on the neurological,[1–4] reproductive,[3,5] gastrointestinal,[3] endocrine[3,5] and immune[1–3,6] systems of those who have been exposed. Therefore, the efficient remediation of these toxins from drinking water is of great importance to the global community.

A wide variety of water purification techniques have been employed such as filtration, distillation and chemical purification. Many of these processes are optimized for large scale purification at water treatment plants, making them difficult to adapt for consumer use. Furthermore, when the infrastructure that carries the water to consumers is the source of the pollution, as is the case in Flint, Michigan, these industrial scale processes are ineffective. In low-income areas where this type of pollution often persists, not only cost but decrepit infrastructure is a major barrier to clean water.

In order to address these challenges, we report a shear-thinning hydrogel composition made from chitosan and diacrylated Pluronic F-127 (DAP), a photo-crosslinkable polyether that can be 3D printed into custom shapes. Chitosan, a polysaccharide derived from chitin, is the main component found in crustacean shells and a known biocompatible, biodegradable and cost-effective material.[6–9] Due to these appealing features, it has found applications in the biomedical,[10,11] regenerative engineering,[12,13] dental[14] and pharmaceutical[15] fields. Its structure contains lone electron pairs on the amine nitrogen atoms and hydroxyl groups, which can act as chelating sites for heavy metal ions.[16] Previous work has used modified chitosan for the removal of dyes and metal ions from water sources;[6,8,17–23] however, these previous examples suffered from poor processability, which also led to poor reusability.[24] While chitosan possesses the functionality necessary for metal chelation, it is not easily processed into free standing objects on its own. By combining chitosan with DAP, we can render it compatible with inexpensive extrusion-based 3D printing techniques (*ca* US$1000). Unlike injection molding, 3D printing allows for objects with complex internal structures to be produced that have increased surface area. Herein, we describe cost-effective, reusable and 3D printable adsorbent materials which can be printed into objects featuring greater surface areas that cannot be achieved through injection molding. We go further and demonstrate that the improved surface areas greatly aid the removal of toxic heavy metal ions from contaminated water.

* *Correspondence to: JJ Gassensmith or RA Smaldone, Department of Chemistry and Biochemistry, University of Texas at Dallas, Richardson, TX, USA. E-mail: gassensmith@utdallas.edu (Gassensmith); ronald.smaldone@utdallas.edu (Smaldone)*

Department of Chemistry and Biochemistry, University of Texas at Dallas, Richardson, Texas,, USA

EXPERIMENTAL

Materials

All chemicals were used as received without further purification. Chitosan powder (85% deacetylated, viscosity average molecular weight *ca* 100–300 kDa), acryloyl chloride and sodium bicarbonate were purchased from Alfa Aesar, Ward Hill, MA, USA. Pluronic F-127 (average molecular weight 12.5 kDa) was supplied by Spectrum Chemical Corporation, New Brunswick, NJ, USA. Irgacure-754 was purchased from BASF Corporation, Kaisten, Switzerland. Inductively coupled plasma mass spectrometry (ICP-MS) standards for Cu, Cd, Pb and Hg (1000 ppm in nitric acid), Cu(II) nitrate trihydrate, Pb(II) nitrate and Hg(II) nitrate monohydrate were purchased from Sigma-Aldrich, St. Louis, MO, USA. Cd(II) nitrate tetrahydrate was supplied by Fisher Scientific, Waltham, MA, USA. Glacial acetic acid, dichloromethane, anhydrous diethyl ether and anhydrous sodium sulfate were supplied by Fisher Chemical, Hampton, NH, USA. Triethylamine was purchased from Acros Organics, Waltham, MA, USA. Ultrapure water (18.2 Ω) was obtained from an Elga PURELAB Flex2 water purification system. Metal concentrations were analyzed using an Agilent 7900 inductively coupled plasma mass spectrometer under helium mode. All ICP-MS measurements were carried out using an aqueous solution containing 3% nitric acid and 2% hydrochloric acid as the matrix. Each measurement was calculated as an average of three measurements.

Synthesis of DAP[25]

Pluronic F-127 (12.6 g, 1 mmol) was dissolved in anhydrous dichloromethane (50 mL). This solution was placed in an ice bath and triethylamine (0.99 mL, 6 mmol) was added followed by acryloyl chloride (0.48 mL, 6 mmol) dropwise over 30 min; the reaction was stirred for 24 h. The crude product was extracted using dichloromethane (450 mL) followed by washing with deionized water (50 mL), saturated sodium bicarbonate aqueous solution (50 mL) and again with deionized water (50 mL). Once the organic phase was collected and dried over anhydrous sodium sulfate, the solvent was removed under reduced pressure. The obtained crude product was re-dissolved in dichloromethane (50 mL), cooled in an ice bath and precipitated as a white solid by the addition of diethyl ether. The final product was collected by filtration as a white solid and dried at 40 °C under vacuum for 24 h. Yield 10.2 g, 80%. ^{1}H NMR (Fig. S1) (600 MHz, deuterated dimethyl sulfoxide) δ 6.34 (d, $J = 12$ Hz, CH_2), 6.2 (dd, $J = 9$, 12 Hz, CH), 5.97 (d, $J = 9$ Hz, CH_2).

Synthesis of hydrogels

Hydrogel compositions containing 1, 5 and 10 wt% chitosan with 9 wt% DAP (cDAP-1, cDAP-5, cDAP-10 respectively) were prepared as follows. Chitosan powder was added to an acetic acid solution (0.06 mol L^{-1}) in ultrapure water. The mixture was heated at 50 °C for 15 min to achieve a homogeneous solution. To this, DAP was added. After adding Irgacure-754 (1 µL) the mixture was gently stirred at 4 °C for 5 h to obtain a homogeneous solution. This solution was then incubated at 37 °C for 5 h to promote gelation. The hydrogel containing 1 wt% chitosan with 25 wt% DAP (cDAP-1X) was prepared in a similar manner. The control, DAP (26 wt%), was prepared as follows. DAP powder was added to an acetic acid solution (0.06 mol L^{-1}) in ultrapure water. Irgacure-754 (1 µL) was added and the mixture was gently stirred at 4 °C for 5 h to obtain a homogeneous solution. This was then incubated at 37 °C for 5 h to promote gelation (Fig. 1).

3D printing

For 3D printing of thin hydrogel sheets, the three hydrogels cDAP-1, cDAP-5 and cDAP-10 were used along with DAP. These were kept at 4 °C for 1 h to obtain the solution state. Each solution was then poured separately into a plastic syringe (60 mL) compatible with a direct-write 3D printer (Printrbot Simple Metal), equipped with a 0.9 mm diameter blunt tip needle. The gel state was obtained by incubating the solutions in the syringes at 37 °C for 1 h. After confirming a homogeneous hydrogel with no trapped air bubbles, the syringe was capped, loaded into the 3D printer, and the hydrogels were printed into sheets having dimensions (length l × width w × height h) 15.0 mm × 15.0 mm × 1.0 mm with four inner circles each of 4.0 mm diameter (Fig. 2(a)). For the 3D printing of hydrogel cups, cDAP-1X and DAP were used. Cylindrical cups with dimensions (outer diameter d × height h × wall thickness t) 25.0 mm × 20.0 mm × 2.0 mm and a base height of 1.5 mm were 3D printed as above (Fig. 2(b)). Solid cubes and shapes with internal structure of the same weight but varying surface area were also 3D printed using cDAP-1X and DAP. Solid cubes with dimensions ($l \times w \times h$) 14 mm × 14 mm × 14 mm, estimated surface area 1176 mm^2; complex shape A having dimensions ($l \times w \times h$) 25 mm × 10 mm × 10 mm, cylindrical pore diameter (d) 5 mm, estimated surface area 1554 mm^2; and complex shape B with dimensions ($l \times w \times h$) 17.5 mm × 10.1 mm × 17.5 mm, cylindrical pore diameter (d) 5 mm, estimated surface area 1791 mm^2 were 3D printed (Fig. 2(c)). The detailed printing conditions for all the structures are given in Tables S1–S3.

UV curing

Each 3D printed structure was subjected to UV curing at 365 nm under 4 W power for 1 h in a UV oven.

RESULTS AND DISCUSSION

In shear-thinning hydrogels, the viscosity of the gel decreases under shear strain, which is a property that can be exploited in extrusion-based 3D printing applications to produce free standing objects without the need for heating or additional chemical reactions. For effective 3D printing, both consistent extrusion under pressure and inter-layer adhesion to the previously printed layers are required. We observed that the extrudable, shear-thinning hydrogels formed by chitosan and DAP fulfilled these criteria. In order to determine the optimal chitosan-DAP (cDAP) mixture for good printability, we prepared the hydrogel compositions shown in Table 1.

The hydrophilic chitosan molecules (colored red in Fig. 1) embed themselves in the DAP matrix in contact with its hydrophilic

Table 1. Hydrogel compositions used in this study; each formulation also contains acetic acid (0.06 mol L^{-1})

Hydrogel	Chitosan (wt%)	Diacrylated Pluronic (wt%)	Ultrapure water (wt%)
cDAP-1	1	9	90
cDAP-5	5	9	86
cDAP-10	10	9	81
cDAP-1X	1	25	74
cDAP-5X	5	25	70
cDAP-10X	10	25	65
DAP	0	26	74

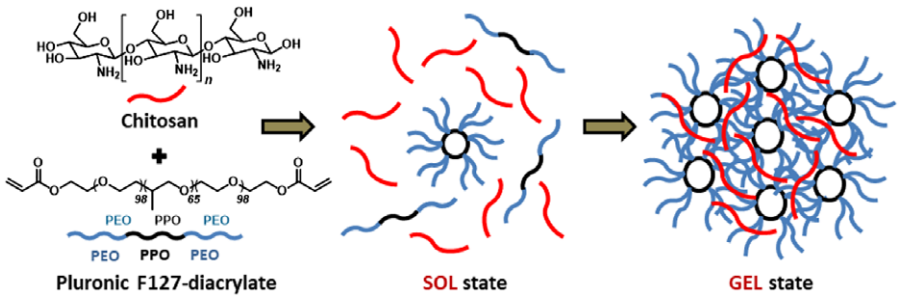

Figure 1. Schematic illustration of chitosan/Pluronic diacrylate hydrogels. At low temperatures (4 °C), chitosan and DAP molecules are evenly distributed forming a homogeneous solution, the 'sol' state. When the temperature of the solution is increased to room temperature, the DAP molecules arrange into micelles trapping chitosan in the 'gel' state.[26]

poly(ethylene)oxide component (colored blue) resulting in stable hydrogels (Fig. 1).[27]

The cDAP can then be loaded directly into a gel extrusion printer as a liquid when the temperature is below the critical micelle concentration (<4 °C). The solution was allowed to warm to room temperature resulting in the gel state which could be used to form the various 3D printed shapes (illustrated in Fig. 2) via direct-write printing.[28,29] Direct-write printing is a cheap and versatile layer-by-layer fabrication method similar to fused filament fabrication.[30–33] Initially, we printed thin sheets consisting of single layers of gel deposition (Fig. 2(a)). We observed increasing surface roughness and inhomogeneity as the amount of chitosan was increased in the blend. As we attempted to print more complex shapes, it became clear that the cDAP-5 and cDAP-10 mixtures could not be printed into shapes with more than one layer of height as they lacked sufficient mechanical strength to be free standing (cDAP-1) or were not sufficiently shear thinning to flow smoothly (cDAP-5, cDAP-10). We increased the amount of DAP in the cDAP formulation in an attempt to create free standing structures during the printing process. While increasing the amount of DAP in each cDAP formulation improved the gel stiffness and printability (cDAP-1X), we also observed poor hydrogel flow when the total chitosan content was increased (cDAP-5X and cDAP-10X), which led to poor print resolution and layer adhesion (Fig. 2(b)).

Based on these tests, cDAP-1X was identified as the most printable formulation for filter fabrication. Using this cDAP-1X formulation, we were also able to print several designs, including solid cubes, cups and objects with internal structure that could not be fabricated easily using conventional molding techniques (Fig. 2(c)).

Evaluation of hydrogel mechanical properties

To quantify the effects that chitosan has on the gel blends, compression tests were carried out for the cured cups, using a universal testing machine (Instron 5848 MicroTester) at a compression rate of 5 mm min^{-1} and a temperature of 25 °C. Ultimate strength, toughness and Young's modulus values were each determined as averages from three measurements (Tables S4–S5).

All the resulting mechanical properties, ultimate strength, toughness and Young's modulus, had been improved in the cDAP-1X compared with the control DAP cups (Fig. 3). This could be attributed to the stabilization of cDAP-1X via inter- and intra-molecular hydrogen bonds.

Maximum metal adsorption tests of DAP and cDAP sheets

Adsorption experiments were carried out in order to determine the maximum concentration of metal ion that can be removed from solution by each adsorbent hydrogel (Fig. 4).

3000 ppb stock solutions (5 mL) were prepared using the nitrate salts of the heavy metals in ultrapure water. Polyethylene terephthalate scintillation vials (20 mL) were used as containers for all the experiments. The sheets (20 mg) were soaked in these solutions (5 mL) on an orbital shaker plate at a rate of 60 rpm, at pH 7, for 1, 3, 5, 7 and 9 h at room temperature to determine the maximum adsorption of each heavy metal. After each time interval, the used adsorbents were washed with aqueous acid (HNO_3, 1 mol L^{-1}) solution (5 mL) for 24 h to extract any adsorbed metal into solution. Each of these solutions were diluted 10× with ultrapure (18.2 MΩ) water. The metal concentrations were analyzed using ICP-MS. The maximum adsorption of each heavy metal was plotted in parts per billion of metal ion adsorbed from solution per 20 mg of dry hydrogel by measuring the amount of metal adsorbed in each hydrogel at different time points (Table S6, Fig. S2). Each adsorption value was obtained as an average from three measurements. Using these isothermal adsorption plots, the maximum adsorption of each heavy metal was calculated as milligrams of metal per gram of dry hydrogel as shown in Fig. 4. The sheets (cDAP-1, cDAP-5 and cDAP-10) show a trend in total adsorption of $Pb^{2+} > Cu^{2+} > Cd^{2+} > Hg^{2+}$. Intuitively, cDAP-10 sheets have the highest metal ion adsorption (*ca* 0.6–0.5 mg metal (g of dry hydrogel)$^{-1}$); however, cDAP-1 was capable of absorbing *ca* 70% as much as cDAP-10 while retaining its printability.

Metal adsorption tests of DAP and cDAP cups

The main goal in this work was to test the heavy metal chelation ability of 3D printed cDAP-1X and evaluate the purity of treated water against the US Environmental Protection Agency (EPA) recommended action level,[34] which is defined as the maximum level of pollutant concentration considered to be safe.

We 3D printed cup-shaped containers which were filled with aqueous solutions of each metal ion in concentrations that represent moderately polluted water bodies.[35,36] For the detection of Cu^{2+} levels, a 1500 ppb Cu^{2+} stock solution (5 mL) was prepared using the nitrate salt in ultrapure water and added to the cups, each of which contained 3 g of dry hydrogel, followed by shaking as before at pH 7.0 and room temperature for 30, 60, 90 and 120 min. After each time period, the supernatant was analyzed via ICP-MS (Fig. 5). To detect Cd^{2+} and Pb^{2+} levels the same procedure was carried out but using 30 ppb stock solutions, Hg^{2+} levels with a 10 ppb stock solution, prepared using the corresponding metal nitrate salt. cDAP-1X cups showed significantly larger adsorption compared to DAP, reducing the concentration of each metal below the EPA action level after only 30 min of contact time.

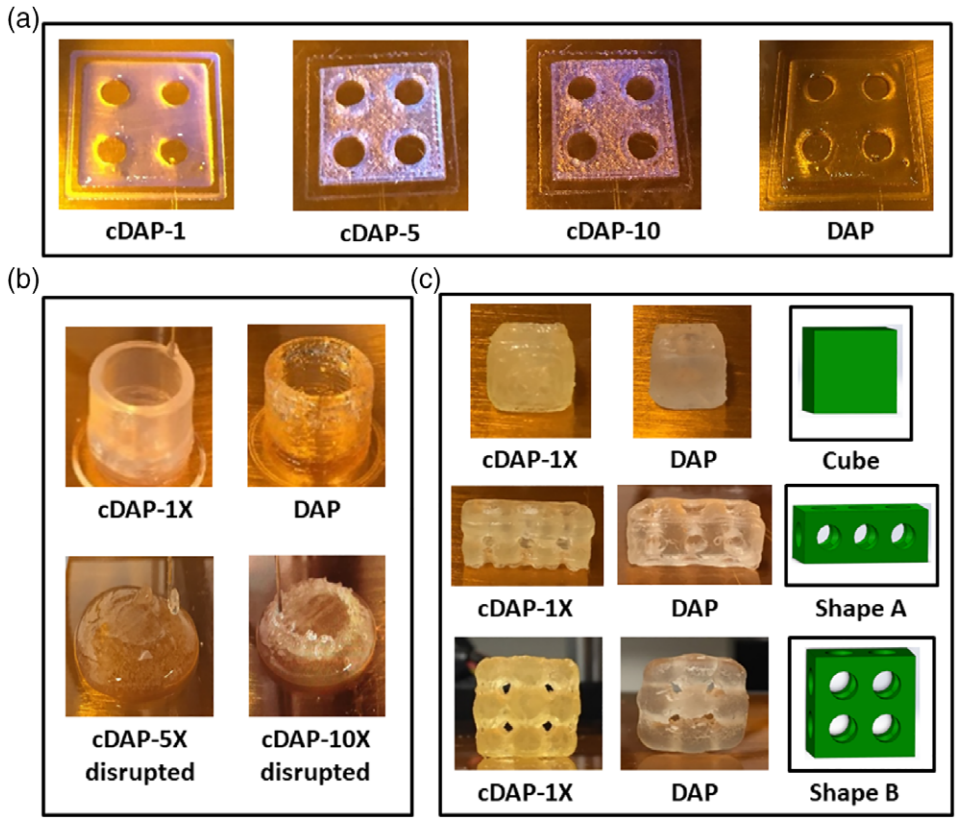

Figure 2. Images of 3D printed hydrogels: (a) thin sheets; (b) cups; note the reduced printability when the chitosan content is increased; (c) solid cubes, shapes A and B with internal structure, and their corresponding renderings.

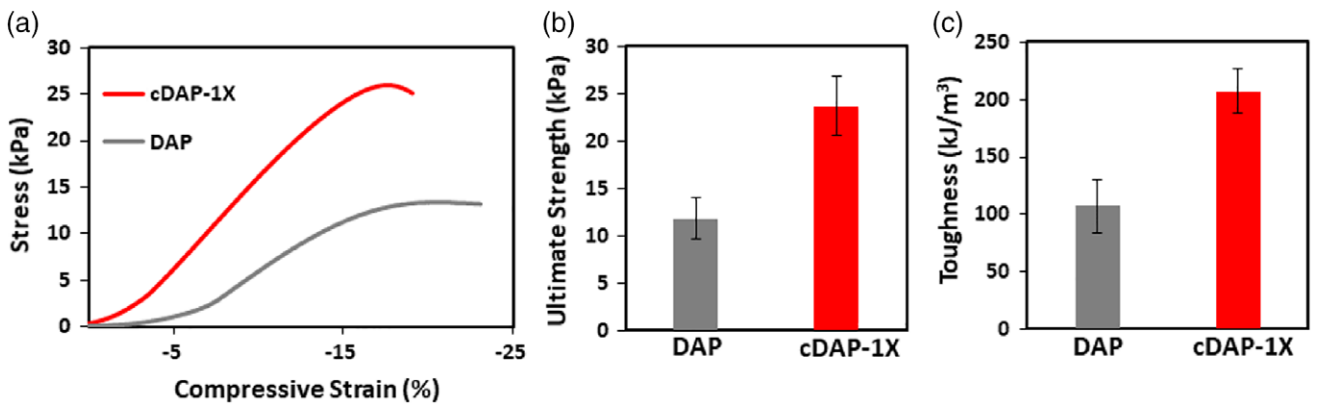

(d)

Material	Young's Modulus (kPa)
cDAP-1X	1.93 ± 0.06
DAP	1.24 ± 0.06

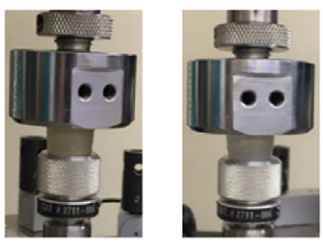

Figure 3. Mechanical characterization of hydrogel cups. (a) Representative stress *versus* strain plots, (b) ultimate strength and (c) toughness values for cDAP-1X and DAP. (d) Young's moduli tabulated along with an illustration of the two materials under compressive stress. *t* tests demonstrate a statistical significance of $p < 0.05$ for these measurements (Table S18).

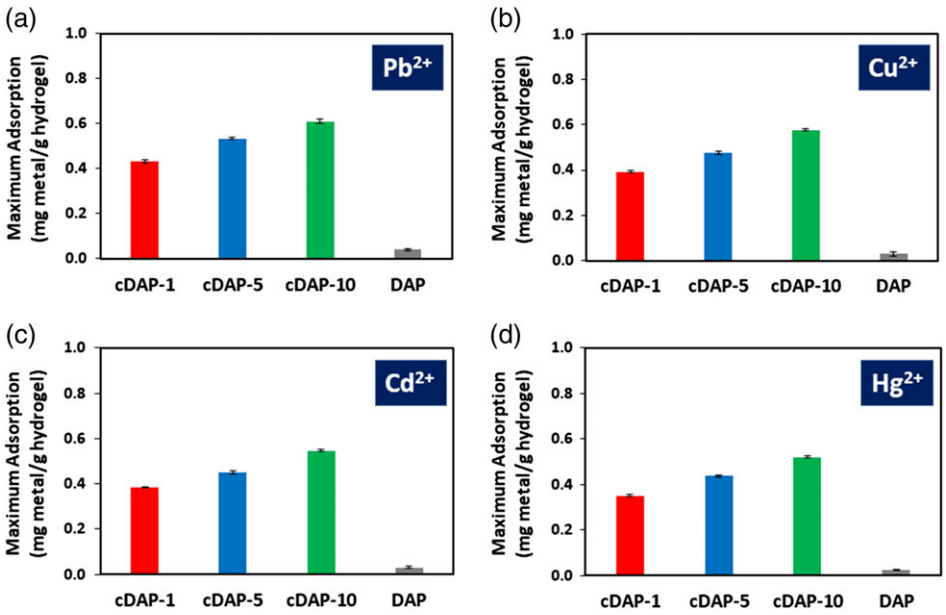

Figure 4. Maximum heavy metal adsorptions of the sheets cDAP-1, cDAP-5, cDAP-10 and DAP. *t* tests demonstrate a statistical significance of $p < 0.05$ for these measurements. Metal adsorptions were shown in both mg of metal/g hydrogel and ppb/20 mg hydrogel (Tables S19–S26).

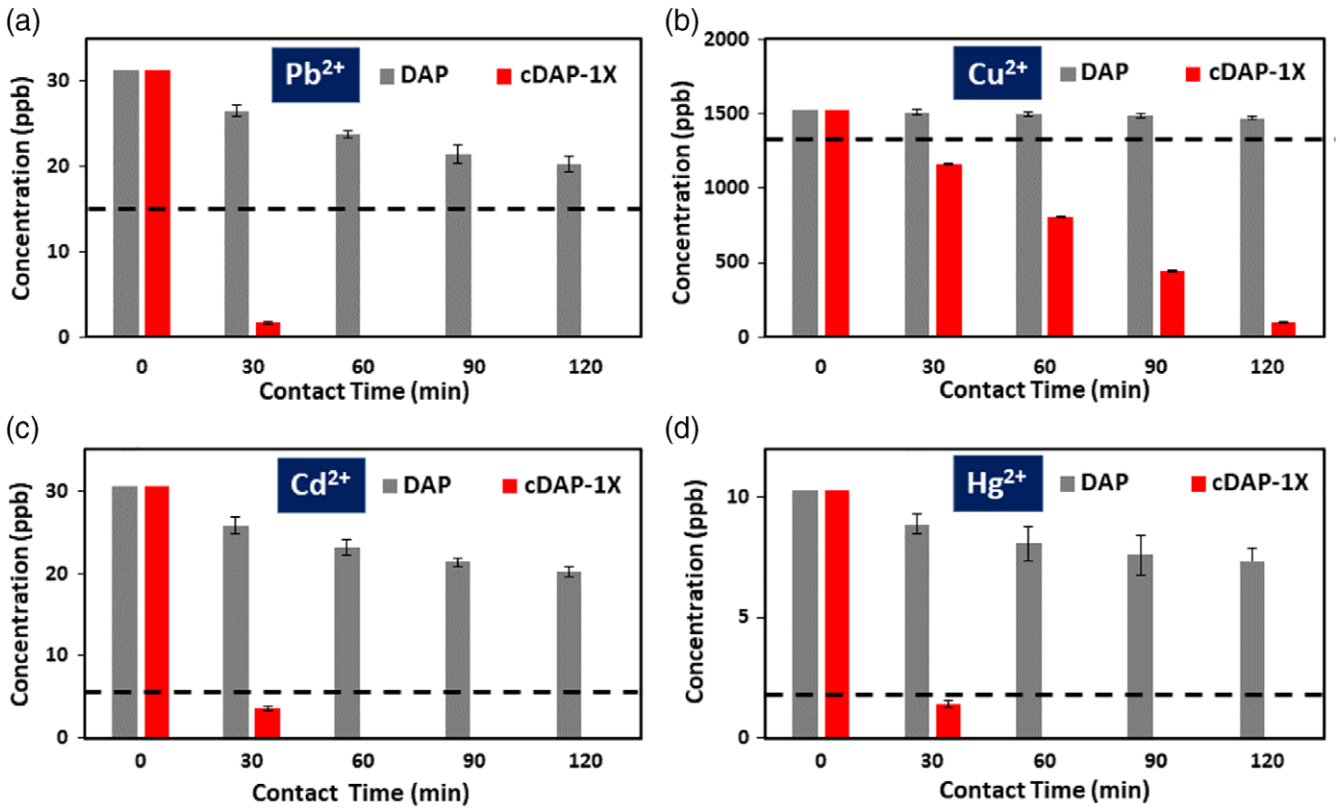

Figure 5. Comparison of remaining heavy metal ion concentrations in solution for cDAP-1X and DAP. EPA action levels are shown as dotted lines. A contact time of 0 min represents the initial heavy metal ion concentration in the stock solution. cDAP-1X data points for Pb, Cd and Hg after 30 min were below the detection limit of the ICP-MS (Tables S7–S10).

Metal leaching tests of DAP and cDAP cups

Leaching tests were also carried out to further evaluate the metal chelation efficiency of the hydrogel cups (Tables S11–S15). The cups that were used in the previous adsorption experiments were used here as well. Ultrapure water (5 mL) was added into the metal loaded cups and shaken as previously described for 10 h at room temperature. The supernatant was then analyzed for metal content by ICP-MS (Fig. 6). The metal concentrations were obtained as averages from three measurements and were calculated as a percentage of the initially adsorbed amounts. As

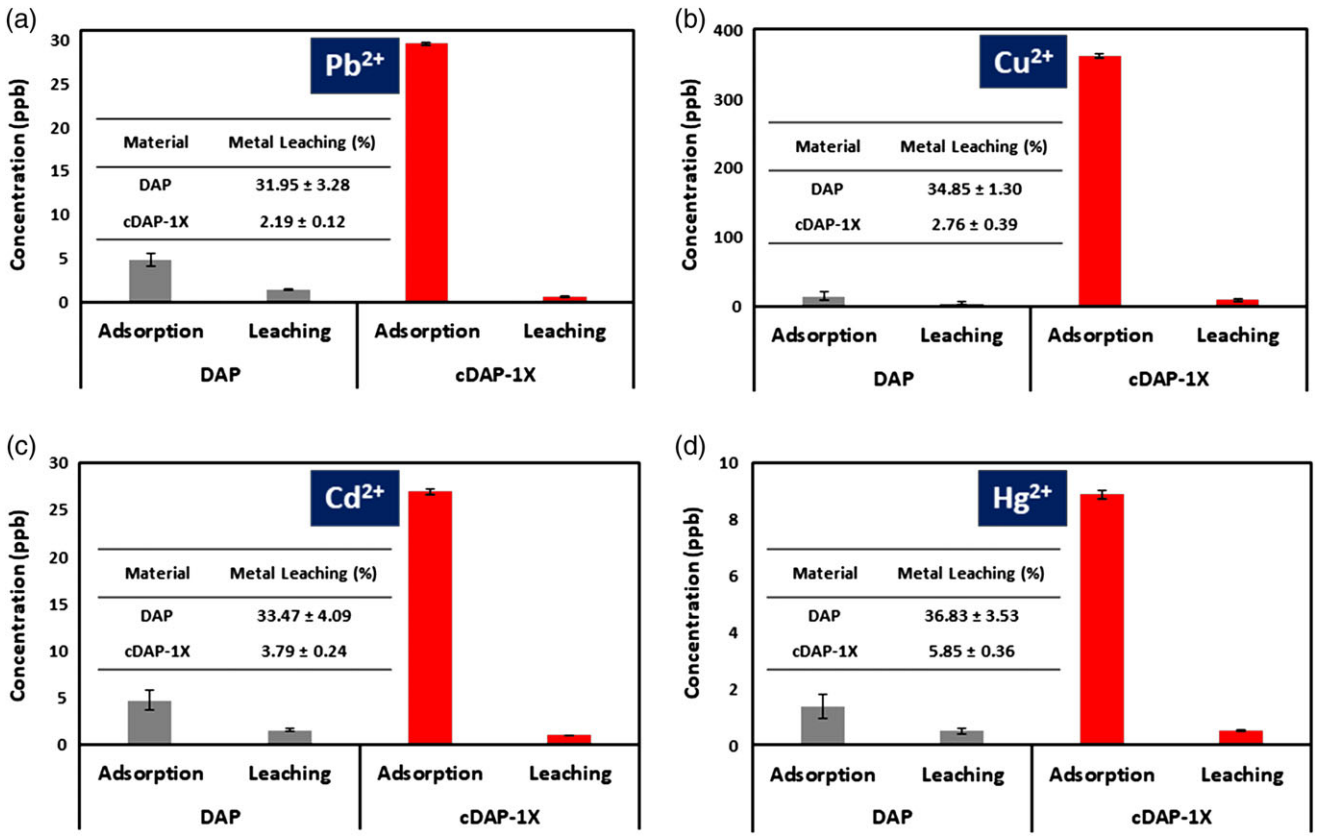

Figure 6. Concentrations of leached metals after 10 h *versus* initially adsorbed amounts for cDAP-1X and DAP after 30 min initial contact time. Metal leaching as a percentage of the initially adsorbed amount is tabulated inside each plot. *t* tests demonstrate a statistical significance of $p < 0.05$ for these measurements (Table S27).

shown in Fig. 6, cDAP-1X cups showed significantly low leaching for all metal ions compared to the control DAP after a contact time of 10 h.

Pb^{2+} adsorption versus hydrogel surface area

One major advantage of using 3D printing is the ability to produce objects with complex internal geometry and higher surface area compared to traditional manufacturing techniques like injection molding or blow molding. A higher surface area in a filtration device allows for greater flux through the adsorbent requiring less pressure and energy during purification. Pb^{2+} can leach from plumbing systems of public water supplies[34] and is the most common metal pollutant in drinking water of the four metals tested here. In order to evaluate the effects of surface area on the adsorption kinetics, we carried out tests using aqueous solutions of Pb^{2+} ions (Table S16, Fig. 7(a)) using shapes consisting of cDAP-1X with different amounts of accessible surface area (Fig. 7(b)). These shapes (2 g dry hydrogel) were submerged in 30 ppb $Pb(NO_3)_2$ stock solutions (5 mL) in ultrapure water and shaken for 10 min at room temperature. The remaining Pb^{2+} in each solution was measured with ICP-MS (Fig. 7(a)).

According to these results, Pb^{2+} removal efficiency is improved with increasing surface area. The cDAP-1X shape B, which has the highest surface area (1791 mm^2), is capable of removing *ca* 74% of the Pb^{2+} ions after 10 min, *ca* four times more than that of its DAP counterpart. This is consistent with our hypothesis that greater surface area to volume ratio of the adsorbent material would improve the metal adsorption kinetics.

Reusability tests

We tested the cDAP-1X shape B for its reusability (Table S17, Fig. 8(a)). The used adsorbent was first washed with an aqueous HCl (1 mol L^{-1}) solution (5 mL) until no more Pb ions were detected, followed by neutralization with an aqueous NaOH (0.1 mol L^{-1}) solution (5 mL) several times and ultrapure water until the pH of the filtrate was 7. The adsorbent was then subjected to Pb^{2+} adsorption again by soaking in 30 ppb stock solution (5 mL) in ultrapure water and placed on a shaker at room temperature for 10 min. The remaining Pb^{2+} level was measured using ICP-MS. This procedure was repeated five times.

We observed that *ca* 98% recovery of the original Pb^{2+} removal efficiency could be achieved even after five cycles. Figure 8(b) also illustrates how the cDAP-1X shape B retains its structure after undergoing several washes in both acidic and basic solutions during the regeneration cycles. Previous literature reports[25,27,37–39] have demonstrated the morphological stability of similar types of hydrogel materials with varying pH. These literature reports support our observations that the cDAP materials will be structurally stable throughout the pH changes experienced during the water purification process.

CONCLUSION

In conclusion, we have designed recyclable, 3D printable materials from a cheap, abundant biopolymer for the remediation of toxic heavy metal ions in water. Using these cDAP materials, we were able to successfully prepare 3D printed objects including sheets, cups and objects with more complex internal structures, which

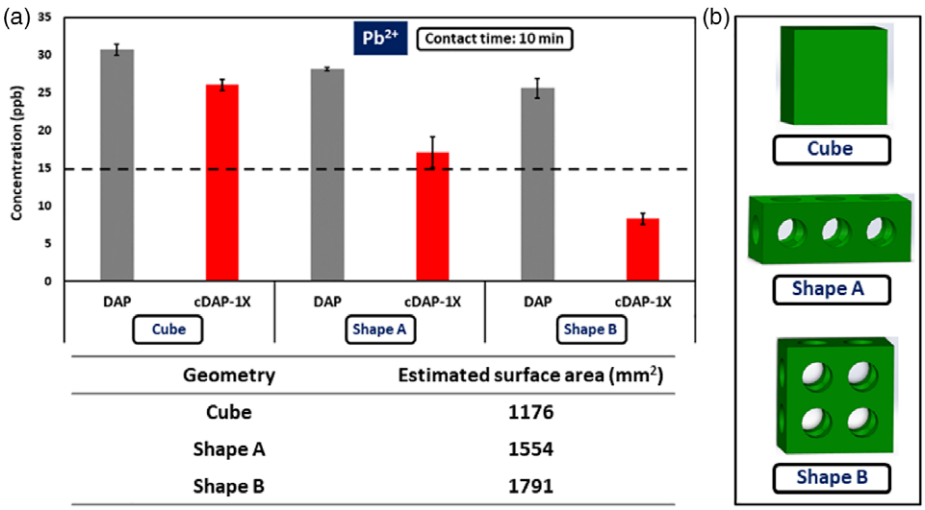

Geometry	Estimated surface area (mm^2)
Cube	1176
Shape A	1554
Shape B	1791

Figure 7. (a) Pb adsorption tests on different shapes (2 g) after a 10 min contact time and their estimated surface areas. Initial Pb^{2+} concentration was 30 ppb. (b) Computer renderings of each shape.

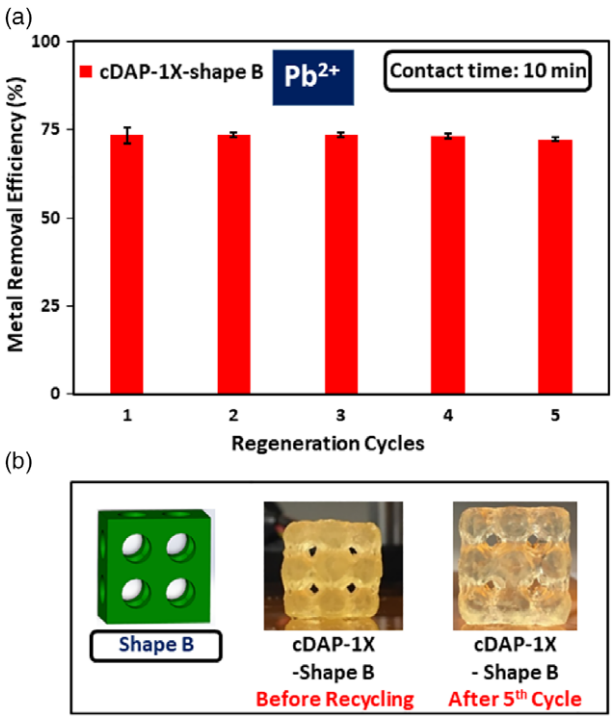

Figure 8. (a) Pb^{2+} removal efficiency (%) for cDAP-1X shape B hydrogel during five regeneration cycles with a contact time of 10 min in each. (b) Illustration of the adsorbent shape before use and after the fifth regeneration cycle. *t* tests demonstrate no statistical significance of $p > 0.05$ for these measurements (Table S28) indicating a very high percentage recovery of the original Pb^{2+} removal efficiency in later cycles.

would be difficult to obtain via conventional molding techniques. Moreover, this novel and cost-effective approach to remove health and environmental hazards could be useful for fabricating cheap and safe water filtration devices on site in polluted areas without the need for industrial scale manufacturing tools.

AUTHOR CONTRIBUTIONS

The paper was written through contributions of all authors. All authors have given approval to the final version.

ACKNOWLEDGEMENTS

R.A.S. acknowledges the University of Texas, Dallas, and the US Department of Energy, National Nuclear Security Administration, managed by Honeywell FM&T (N000263171), for funding. J. J. G. acknowledges the National Science Foundation (DMR-1654405) for funding.

CONFLICTS OF INTEREST

There are no conflicts of interest to declare.

SUPPORTING INFORMATION

Supporting information may be found in the online version of this article.

REFERENCES

1 Alghanmi RM, *E-J Chem* **9**:1007–1016 (2012).
2 Anh NTN, Chowdhury AD and Doong R, *Sens Actuators B Chem* **252**:1169–1178 (2017).
3 Tchounwou PB, Yedjou CG, Patlolla AK and Sutton DJ, *Mol Clin Environ Toxicol* **101**:133–164 (2012).
4 Worthington MJH, Kucera RL, Albuquerque IS, Gibson CT, Sibley A, Slattery AD *et al.*, *Chem Eur J* **23**:16219–16230 (2017).
5 Rana SVS, *Biol Trace Elem Res* **160**:1–14 (2014).
6 Wan NWS, Teong LC and Hanafiah MAKM, *Carbohydr Polym* **83**:1446–1456 (2011).
7 Józef N, Małgorzata T and Konrad W, *Chem Process Eng* **37**:485–501 (2016).
8 Thakur VK and Thakur MK, *ACS Sustain Chem Eng* **2**:2637–2652 (2014).
9 Varma AJ, Deshpande SV and Kennedy JF, *Carbohydr Polym* **55**:77–93 (2004).
10 Balan V and Verestiuc L, *Eur Polym J* **53**:171–188 (2014).
11 Lai P, Daear W, Löbenberg R and Prenner EJ, *Colloids Surf B Biointerfaces* **118**:154–163 (2014).
12 Jiang T, Deng M, James R, Nair LS and Laurencin CT, *Acta Biomater* **10**:1632–1645 (2014).
13 Croisier F and Jérôme C, *Eur Polym J* **49**:780–792 (2013).
14 Wieckiewicz M, Boening WK, Grychowska N and Paradowska-Stolarz A, *Mini Rev Med Chem* **17**:401–409 (2017).
15 Islam S, Bhuiyan MAR and Islam MN, *J Polym Environ* **25**:854–866 (2017).
16 Wu F, Tseng R and Juang R, *J Hazard Mater* **81**:167–177 (2001).
17 Ma J, Zhou G, Chu L, Liu Y, Liu C, Luo S *et al.*, *ACS Sustain Chem Eng* **5**:843–851 (2017).

18 Li N and Bai R, *Ind Eng Chem Res* **44**:6692–6700 (2005).
19 Zhao F, Repo E, Sillanpää M, Meng Y, Yin D and Tang WZ, *Ind Eng Chem Res* **54**:1271–1281 (2015).
20 Chen A, Liu S, Chen C and Chen C, *J Hazard Mater* **154**:184–191 (2008).
21 Igberase E, Osifo P and Ofomaja A, *Appl Organomet Chem* **32**:e4131 (2017).
22 Sharma RK, Devi L and Singh A, *Der Pharma Chem* **8**:58–71 (2016).
23 Hu C, Li G, Wang Y, Li F, Guo G and Hu H, *Int J Biol Macromol* **103**:751–757 (2017).
24 Wang J and Chen C, *Bioresour Technol* **160**:129–141 (2014).
25 Yoo HS, *J Biomater Sci Polym Ed* **18**:1429–1441 (2007).
26 Jung Y, Park W, Park H, Lee D and Na K, *Carbohydr Polym* **156**:403–408 (2017).
27 Darabi MA, Khosrozadeh A, Mbeleck R, Liu Y, Chang Q, Jiang J *et al.*, *Adv Mater* **29**:1700533 (2017).
28 Basu A, Saha A, Goodman C, Shafranek RT and Nelson A, *ACS Appl Mater Interfaces* **9**:40898–40904 (2017).
29 Lin Q, Hou X and Ke C, *Angew Chem Int Ed* **56**:4452–4457 (2017).
30 Appuhamillage GA, Reagan JC, Khorsandi S, Davidson JR, Voit W and Smaldone RA, *Polym Chem* **8**:2087–2092 (2017).
31 Davidson JR, Appuhamillage GA, Thompson CM, Voit W and Smaldone RA, *ACS Appl Mater Interfaces* **8**:16961–16966 (2016).
32 Yang K, Grant JC, Lamey P, Joshi-Imre A, Lund BR, Smaldone RA *et al.*, *Adv Funct Mater* **27**:1700318 (2017).
33 Xu W, Pranovich A, Uppstu P, Wang X, Kronlund D, Hemming J *et al.*, *Carbohydr Polym* **187**:51–58 (2018).
34 Tarragó O and Brown MJ, *Case studies in environmental medicine (CSEM), lead toxicity*. Available: https://www.atsdr.cdc.gov/csem/lead/docs/CSEM-Lead_toxicity_508.pdf [23 January 2018].
35 Zhang Z, Wang J, Ali A and Delaune R, *Environ Monit Assess* **188**:628 (2016).
36 Das T and Haldar D, *ACS Omega* **2**:6878–6887 (2017).
37 Lin Q, Li L, Tang M, Hou X and Ke C, *J Mater Chem C* **6**:11956–11960 (2018).
38 Kim KS and Park SJ, *Colloids Surf B Biointerfaces* **80**:240–246 (2010).
39 Choi JS and Yoo HS, *Biomater Sci* **24**:210–223 (2013).

